Study of phonon modes in germanium nanowires

Xi Wang[a] and Ali Shakouri[b]
Baskin School of Engineering, University of California, Santa Cruz, California 95064

Bin Yu, Xuhui Sun, and Meyya Meyyappan
Center for Nanotechnology, NASA Ames Research Center Moffett Field, California 94035

(Received 26 December 2006; accepted 24 May 2007; published online 6 July 2007)

The observation of pure phonon confinement effect in germanium nanowires is limited due to the illumination sensitivity of Raman spectra. In this paper we measured Raman spectra for different size germanium nanowires with different excitation laser powers and wavelengths. By eliminating the local heating effect, the phonon confinement effect for small size nanowires was clearly identified. We have also fitted the Raman feature changes to estimate the size distribution of nanowires. © *2007 American Institute of Physics*. [DOI: 10.1063/1.2752134]

INTRODUCTION

One-dimensional (1D) crystalline structures such as nanowires and nanotubes have been studied extensively during the past several years. Semiconducting nanowires promise applications in future generation electronic and optoelectronic devices. Raman microscopy is a useful tool in the study of quasi-1D materials; it provides information about the surface and volume phonon modes and lattice vibrations, including how those vibrations are affected by extremely small dimensions. Recently, several papers[1–3] have analyzed the Raman peak shifts and the shape of the Raman spectrum for Si nanowires. However, the reported shifts and asymmetric broadenings vary depending on the experimental conditions. Studies show that the optical phonon peaks of silicon nanowires are dependent on the excitation laser power and independent of wavelength. Thus, low laser power is essential in order to examine the phonon spectrum of different size nanowires.[1]

SAMPLE AND EXPERIMENT

Self-assembled single crystalline Germanium (Ge) nanowires allow researchers to observe relatively strong one-dimensional confinement effects for both carriers and phonons. Compared to Si, Ge has smaller electron and hole effective masses and a lower dielectric constant; therefore, nanowires made of Ge should have stronger confinement characteristics than Si nanowires (SiNWs) with the same diameters. The Ge nanowire (GeNW) samples measured in this paper were synthesized through the vapor-liquid-solid[4] (VLS) method on lithographically patterned Au catalyst arrays. The diameters of the synthesized nanowires are 5, 10, and 20 nm, respectively, defined by the catalyst sizes. As a reference, a piece of bulk Ge wafer was also measured in this study. Figure 1 shows scanning electron microscopy (SEM) images of the as-synthesized GeNWs.

During experiment, the ambient temperature was kept at room temperature (22 °C). Experiment was conducted in a clean room to minimize the contaminations. Computer controlled cooling systems were utilized to keep the operation temperature of laser sources and detector stable, and thus to guarantee a stable emission wavelength and detection sensitivity.

RESULTS AND DISCUSSION

We focused a 500 μW Ar^+ laser beam (514.5 nm wavelength) onto the sample surface and collected the scattered light through a monochromater and a charge coupled device (CCD) detector. Results are shown in Fig. 2(a). As one could see, results show the evolution of Raman spectra as a function of diameter D. Significant Stokes peak shift downs, broadenings, and dissymmetries were observed from nanowire Raman spectra in comparing the spectrum from bulk Ge. These changes increase as the nanowire size decreases. Earlier papers[5–7] had reported these phenomena as entirely a contribution of scaling-induced phonon confinement effect. However, when we decreased the excitation laser power, we observed much weaker spectrum changes as a function of nanowire diameter. Figure 2(b) shows the results. In this case, laser power was reduced to 50 μW. Since we kept all other experiment parameters (photon accumulation time, objective magnification, filter setup, etc.) the same, incident laser power difference could become an important factor af-

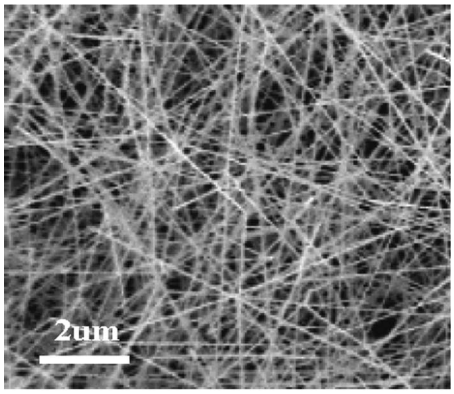

FIG. 1. A SEM image of the as-synthesized GeNW sample.

[a]Electronic mail: wangxi@soe.ucsc.edu
[b]Author to whom correspondence should be addressed; electronic mail: ali@soe.ucsc.edu

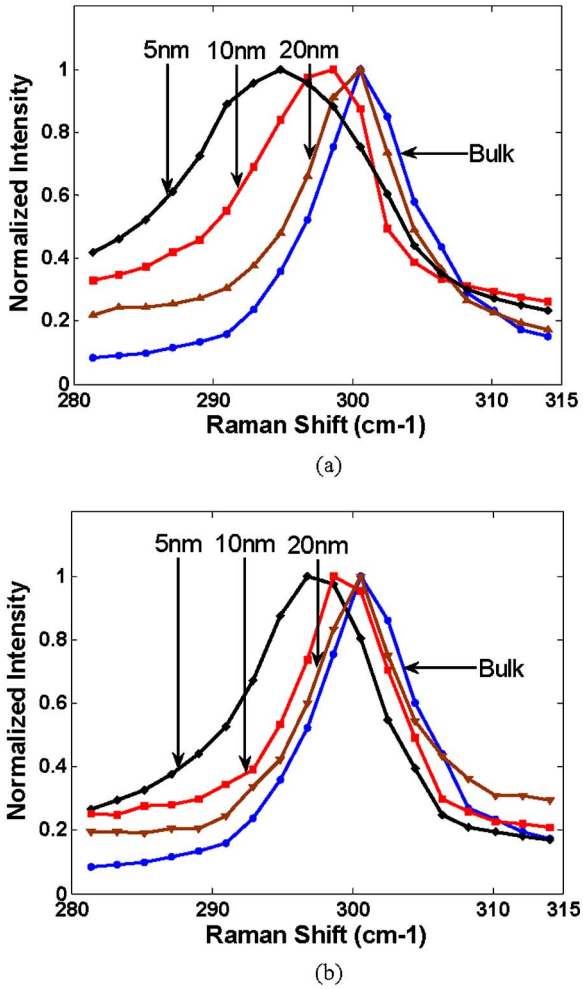

FIG. 2. (Color online) (a) Raman spectra of three GeNW samples (D=5, 10, 20 nm) and bulk Ge measured at 500 uW laser power with 514.523 nm wavelength. (b) Raman spectra of three GeNW samples (D=5, 10, 20 nm) and bulk Ge measured at 50 uW laser power with 514.523 nm wavelength.

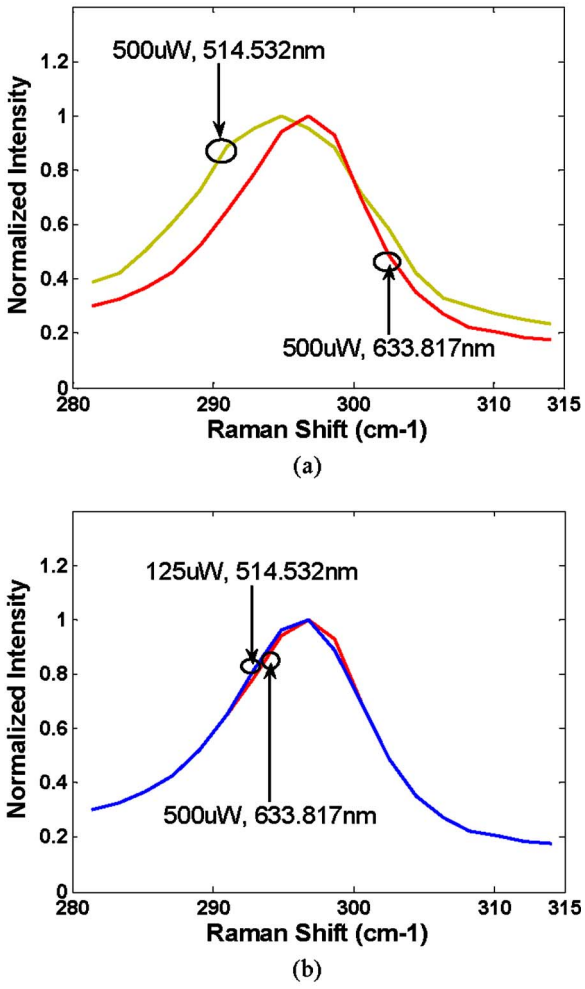

FIG. 3. (Color online) (a) Comparison of Raman spectra of GeNW sample 3 (D=5 nm) measured at 500 μW with 514.532 and 633.817 nm excitation wavelengths. (b) Comparison of Raman spectra of GeNW sample 3 (D=5 nm) measured at 125 μW with 514.532 nm excitation wavelength and 500 μW with 633.817 nm excitation wavelength.

fecting the measured spectra. In other words, pure confinement effect should be looked at only after carefully calibrating and removing this contribution.

Two different excitation lasers, a 514.523 nm Ar^+ laser and a 633.817 nm Kr^+ laser, were used on the four samples to examine their wavelength independency. Figures 3(a) and 3(b) show the results from GeNW sample 3 (D=5 nm), which has the smallest dimension and thus is most sensitive to excitation condition changes. The initial attempt involved exciting the sample with a laser having the same power level (500 μW) but different excitation wavelengths (514.523 and 633.817 nm). The results of this experiment do show an obvious Raman spectrum change. However, it was hard to tell whether this change resulted from a difference in wavelength or a difference in the amount of heat absorbed at different wavelengths. Considering the fact that absorption coefficients of Ge are 600 cm^{-1} for the 514.523 nm Ar^+ laser and 150 cm^{-1} for the 633.817 nm Kr^+ laser, we simply assume that, when applying the same excitation laser power, heat absorbed by Ge samples using a 633.817 nm Kr^+ laser is about $\frac{1}{4}$ that of the same sample using a 514.523 nm Ar^+ laser. Figure 3(b) shows the Raman spectra of GeNW sample 3 (D=5 nm) measured at 125 μW with 514.532 nm excitation wavelength and 500 μW with 633.817 nm excitation wavelength. The remarkable similarities of the Raman features—position, full width at half maximum (FWHM), and asymmetry level—imply that the spectrum changes brought about by differing wavelengths are not due to resonant Raman selection of different size wires, but rather are the results of the absorbed power difference.

To further understand how the incident laser power interacts with the nanowire Raman spectrum, each GeNW sample was excited by a focused laser beam at three different power levels. Measured spectra are shown in Figs. 4(a)–4(c). To achieve a quantized control over the incident laser power, we utilized neutral density filters (NDFs). More specifically, 0, 0.3, and 0.6 density NDFs were inserted between the sample and laser source to indicate 500, 250, and 125 μW pass-through laser powers, respectively, with the original output power equal to 500 μW. As one could see in all three graphs in Fig. 4, incident laser power increase caused the shift downs, broadenings, and dissymmetries in GeNW Raman Stokes peaks, while no significant change can be observed from the bulk Ge Raman spectrum. This is consistent

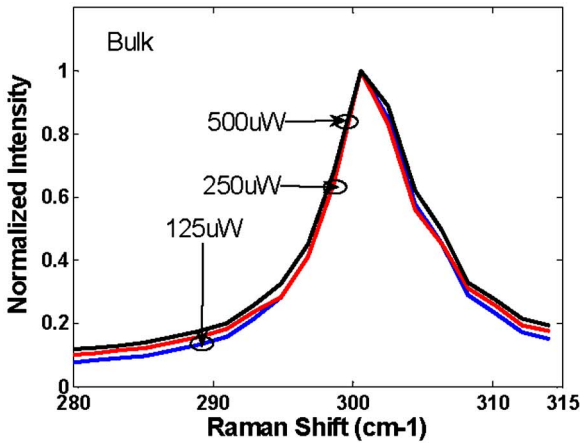

(a)

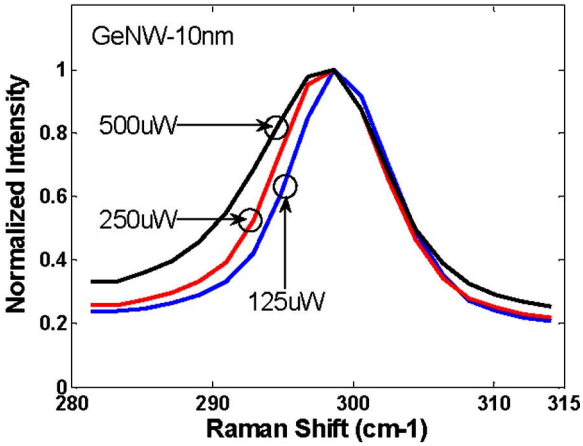

(b)

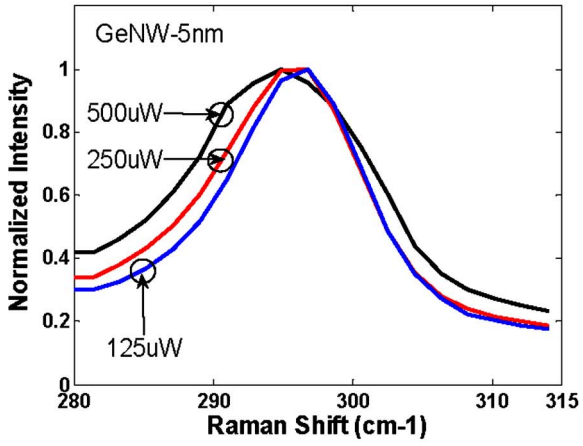

(c)

FIG. 4. (Color online) (a) Raman Stokes peak of bulk Ge with different excitation powers; (b) Raman Stokes peak of 10 nm GeNWs with different excitation powers; (c) Raman Stokes peak of 5 nm GeNWs with different excitation powers.

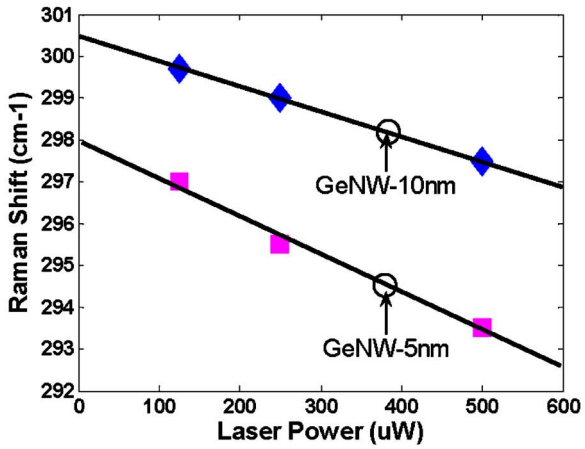

(a)

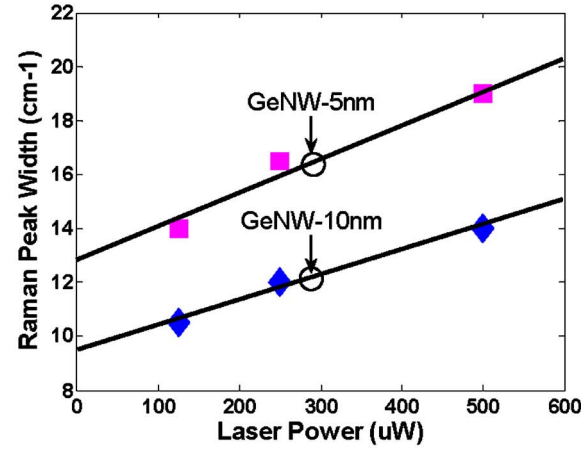

(b)

FIG. 5. (Color online) (a) Raman peak shift of GeNW samples with different excitation powers; (b) Raman peak FWHM of GeNW samples with different excitation powers.

with what has been found in Fig. 1. However, the spectrum obtained from different GeNW samples changes at different rates. Nanowires with smaller diameter respond to incident laser power level change more than the larger diameter nanowires do. This indicates that the incident laser power effect of the nanowire Raman spectrum is sample size sensitive. To explain this phenomenon, one physical mechanism is localized heating at the sample surface caused by the incident laser. The thermal conductivity of semiconductor nanostructures dramatically decreases with size due to the strongly enhanced boundary phonon scattering. Heat would be more easily accumulated in the area that contains smaller size nanostructures, while it would be dissipated faster in the area that contains larger size nanostructures. In bulk material, this amount of heat can be efficiently dissipated to the environment, and therefore causes no effect on the measured Raman spectrum.

In Fig. 5 we show the extracted Raman spectrum changes for the 5 and 10 nm GeNW samples as a function of excitation laser power. With first order fitting, we can get the approximate Raman Stokes peak features (position, peak width) that were contributed by a pure phonon confinement effect. The larger Raman feature changes from smaller diameter nanowires revealed the occurrence of stronger phonon confinement effect.

An estimation of sample local temperature can be obtained by monitoring the Stokes/anti-Stokes intensity ratio,

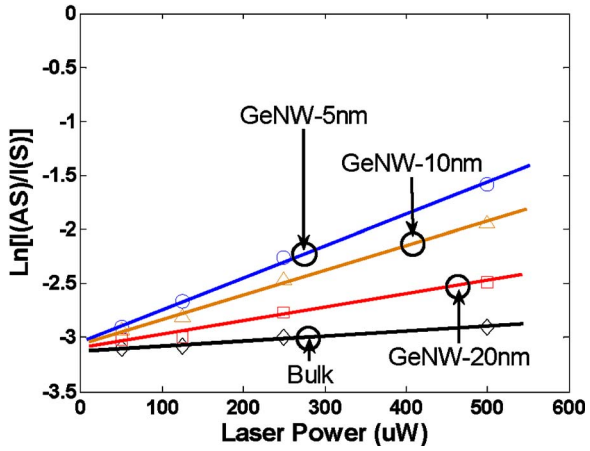

FIG. 6. (Color online) Raman peak ratio as a function of excitation laser power for three GeNW samples (D=5, 10, 20 nm) and bulk Ge measured at 514.532 nm wavelength.

$$\frac{I_{\mathrm{AS}}}{I_{\mathrm{S}}} = \gamma \exp\left(\frac{k_B T}{h\nu}\right), \tag{1}$$

where T is the local temperature on the sample surface, $h\nu$ is the energy gap between excitation and ground phonon energy states, and γ is a coefficient relating to peak position and FWHM. Figure 6 shows the calculated Raman peak ratios as a function of incident laser power for the 5, 10, and 20 nm diameter GeNW samples and bulk Ge. As one could see, localized heating was built up by the highly focused laser beam at the measurement point. Furthermore, local temperature gets higher as the nanowire diameter gets smaller, which coincides with the assumption that more heat would be accumulated in those samples.

Since the density of GeNW was controlled by the density of the lithographically patterned catalyst, it is approximately the same for all samples we used in this study. Therefore the different local heating effect shall come from the size dependent thermal conductivity of nanowires,

$$\kappa = \frac{LQ_{\mathrm{cond}}}{A\Delta T}. \tag{2}$$

Equation (2) is the expression for thermal conductivity, where L represents the thickness of the GeNW layer, Q_{cond} is the amount of heat being conducted, A is the cross-section area through which the heat flows (laser spot size in our case), and ΔT is the local temperature change due to heat flow. From the relationship between Stokes/anti-Stokes intensity ratio and local temperature, we obtained

$$T \propto \ln\left(\frac{I_{\mathrm{AS}}}{I_{\mathrm{S}}}\right). \tag{3}$$

Combining Eqs. (2) and (3), we derive that

$$\kappa \propto \frac{LQ_{\mathrm{cond}}}{A[\ln(I_{\mathrm{AS}}/I_{\mathrm{S}})_1 - \ln(I_{\mathrm{AS}}/I_{\mathrm{S}})_2]} = qr;$$

$$q = \frac{L}{A},$$

$$r = \frac{Q_{\mathrm{cond}}}{[\ln(I_{\mathrm{AS}}/I_{\mathrm{S}})_1 - \ln(I_{\mathrm{AS}}/I_{\mathrm{S}})_2]}. \tag{4}$$

Here q is the dimension ratio of the heat path and r is the absolute slope of each line in Fig. 6. Since we know that κ_b=59.9 W/m−K for intrinsic bulk Ge, we can estimate the GeNW layer thermal conductivity for each sample by using

$$\kappa = \frac{\kappa_b r}{r_b}. \tag{5}$$

The calculated results are 22.8 W/m−K, 12.1 W/m−K, and 9.1 W/m−K for the 20, 10, and 5 nm diameter GeNW samples, respectively, and they indicate different heat conduction capabilities. Since the absorption coefficient of Ge in the measurement wavelength range (514.532–633.817 nm) is significant (0.4–0.25 cm^{-1}), the main part of the incident light is absorbed ($1/e$ penetration depth is 0.025–0.04 μm)[8] far before it reaches the interface between the nanowire layer and substrate, which is about tens of microns beneath the sample surface. The actual small differences among the surface layer thicknesses of each sample do not affect the heat conduction capability estimation. However, they should not be considered as actual thermal conductivities of GeNWs. It is unfortunately difficult to precisely decouple the heat absorbed by wires and the air in between.

To simulate the ideal Raman spectrum for a certain diameter GeNW, we utilized the phonon confinement model of Richter *et al.* and Campbell and Fauchet (RCF),[5,9] in which the Raman intensity is given by

$$I(\omega) = \int \frac{|C(0,q)|^2}{[\omega - \omega(q)]^2 + (\Gamma_0/2)^2} d^3q, \tag{6}$$

where $C(0,q)$ is a Fourier coefficient of the confinement function, $\omega(q)$ is the phonon dispersion, q is the phonon momentum, and Γ_0 is the width (FWHM) of the reference Ge. Considering the basic shape and material of our nanowire samples, we used

$$|C(0,q)^2| = e^{(-q^2D^2/16\pi^2)} \tag{7}$$

and

$$\omega(q) = \sqrt{\{X + Y\cos[q(a/2)]\}} + Z, \tag{8}$$

with X=0.69×10^5 cm^{-2} and Y=0.195×10^5 cm^{-2}. Z is an adjustment parameter for reference samples measured by the same experimental setting in this study, a represents the lattice constant, and D is the diameter of interest of GeNWs. Figure 7 shows the comparison between measurement results and simulation based on the RCF model. Good agreements were obtained for the 20 and 100 nm (bulk) diameter nanowires. However, discrepancy between measurement and simulation differences were found for the 5 and 10 nm diameter nanowires.

Although the diameter of the synthesized nanowire is mainly controlled by the size of the catalysts, a variance still exists due to the nature of self-assembling growth. Therefore, it is good to confirm the actual diameter of the nanowires. Although scanning microscopies, such as atomic force mi-

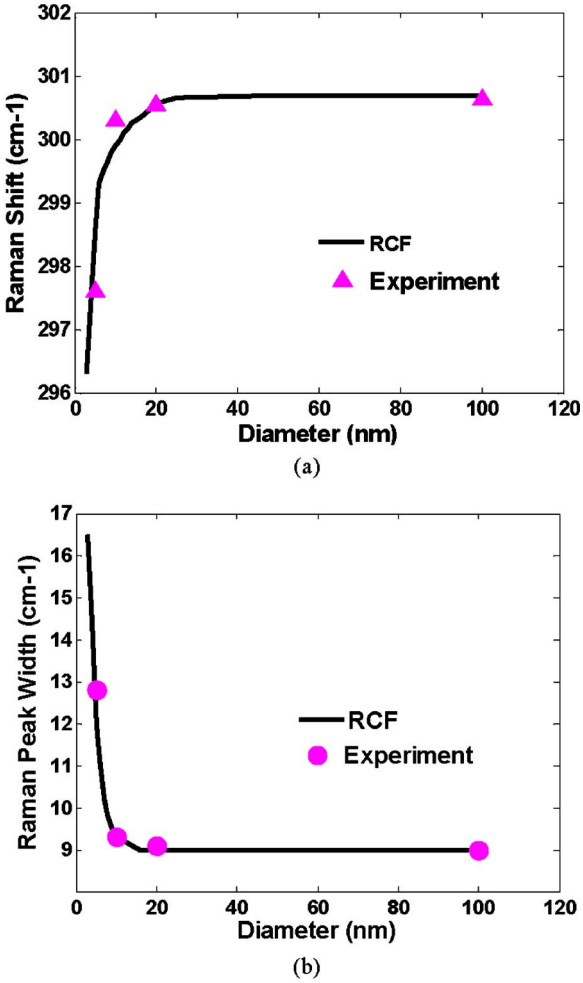

FIG. 7. (Color online) (a) Comparison of Raman shift measured from three GeNW samples (D=5, 10, 20 nm) and bulk Ge to calculation result from the RCF model. (b) Comparison of Raman peak FWHM measured from three GeNW samples (D=5, 10, 20 nm) and bulk Ge to calculation result from the RCF model.

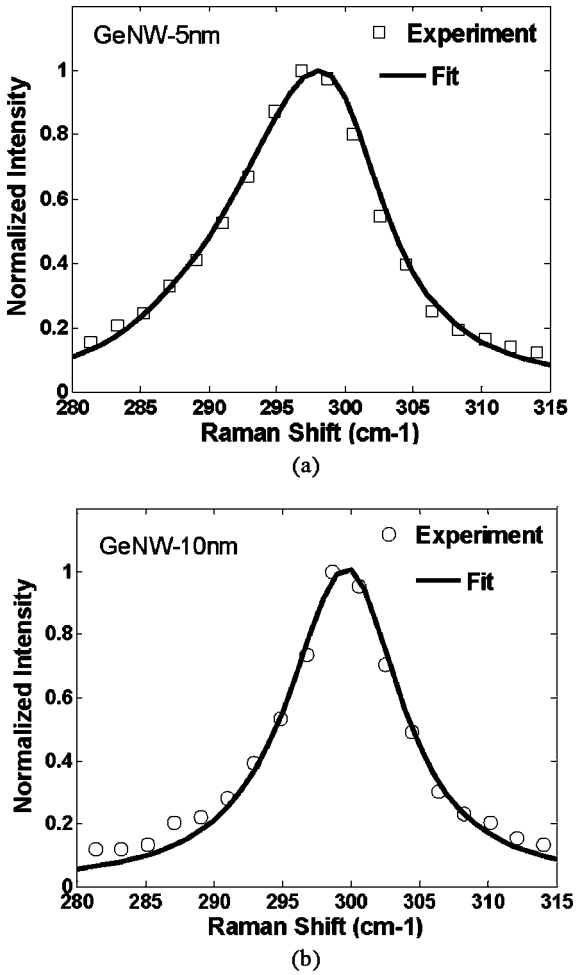

FIG. 8. Dots: Raman spectra of GeNWs measured at 50 μW from (a) sample 3 (D=5 nm) and (b) sample 2 (D=10 nm). Solid line: Fit to the measured spectra using the RCF model adapted for GeNWs. Extracted diameter distributions are (a) 4–5 nm and (b) 7–9 nm.

croscopy (AFM) and SEM, are capable of providing precise dimension information on single nanowires, they could not give size distribution information over a larger amount of similar nanowires.[10–16] Therefore, we fitted the measured Raman spectrum as an integrated result of ideal spectra of nanowires with a range of diameters. If the fitting error is reduced below a certain level, the nanowire size distribution can be approximated. Figures 8(a) and 8(b) show the fitting results. A least-square rule was applied as the fitting criterion. The as-extracted nanowire diameter distributions are 18–19 nm (for D=20 nm sample), 7–9 nm (for D=10 nm sample), and 4–5 nm (for D=5 nm sample). The differences between catalyst sizes and actual nanowire diameters could explain the differences between simulated and measured Raman features in Fig. 8.

CONCLUSION

In conclusion, we have shown the Raman spectra for different size GeNWs by measuring with differing laser powers and wavelengths. The study shows the excitation power dependency and wavelength independency of Raman spectrum evolution. By eliminating the heating of the sample under illumination, we can identify the pure phonon confinement effect for small size nanowires. The fitting of Raman spectra was used to estimate the size distribution of nanowires. The results of GeNW layer conductivity calculation indicated the different heat conduction capabilities of different size GeNWs.

ACKNOWLEDGMENT

This work was supported by NASA Ames, University Affiliated Research Center.

[1]S. Piscanec, A. C. Ferrari, M. Cantoro, S. Hofmann, J. A. Zapien, Y. Lifshitz, S. T. Lee, and J. Robertson, Phys. Rev. B **68**, 241312(R) (2003).
[2]Y. F. Zhang, Y. H. Tang, N. Wang, C. S. Lee, I. Bello, and S. T. Lee, Phys. Rev. B **61**, 4518–4521 (2000).
[3]N. Fukata, T. Oshima, K. Murakami, T. Kizuka, T. Tsurui, and S. Ito, Appl. Phys. Lett. **86**, 213112 (2005).
[4]B. Yu, G. Calebotta, K. Yuan, and M. Meyyappan, NTSI (2005).
[5]I. H. Campbell and P. M. Fauchet, Solid State Commun. **58**, 739–741 (1986).
[6]B. J. Kip and R. J. Meier, Appl. Spectrosc. **44**, 707 (1990).
[7]S. Mathur, H. Shen, V. Sivakov, and U. Werner, Chem. Mater. **16**, 2449–2456 (2004).
[8]H. R. Philipp and E. A. Taft, Phys. Rev. **113**, 1002 (1959).
[9]H. Richter, Z. P. Wang, and L. Ley, Solid State Commun. **39**, 625 (1981).

[10]D. Li, Y. Wu, P. Kim, L. Shi, P. Yang, and A. Majumdar, Appl. Phys. Lett. **83**, 2934 (2003).
[11]A. C. Ferrari, S. Piscanec, S. Hofmann, M. Cantoro, C. Ducati, and J. Robertson, Proceedings of IWEPNM (AIP, Melville, NY, 2003).
[12]R. P. Wang, G. W. Zhou, Y. Liu, S. Pan, H. Zhang, D. Yu, and Z. Zhang, Phys. Rev. B **61**, 16827 (2000).
[13]J. Qi, J. M. White, A. M. Belcher, and Y. Masumoto, Chem. Phys. Lett. **372**, 763 (2003).
[14]M. Malyj and J. E. Griffiths, Appl. Spectrosc. **37**, 315 (1983).
[15]F. LaPlant, G. Laurence, and D. Ben-Amotz, Appl. Spectrosc. **50**, 1034 (1996).
[16]Y. F. Mei *et al.*, Appl. Phys. Lett. **86**, 021111 (2005).